A Hybrid Γ-Model for Distribution Feeders: Linear Parameter Estimation Using Unsynchronized Terminal Measurements

Amin Nassaj, *Student Member*, *IEEE*, Ahmad Salehi Dobakhshari, *Member*, *IEEE*, Vladimir Terzija, *Fellow*, *IEEE*, and Sadegh Azizi, *Senior Member*, *IEEE*

***Abstract*— Accurate estimation of parameters for Distribution Network Feeders (DNFs) is crucial yet quite challenging, especially with limited synchronized measurements. This letter introduces a novel Hybrid Γ-Model (HGM) that leverages the circuit properties of DNFs to establish a linear relationship between unknown feeder parameters and unsynchronized terminal measurements. By combining two symmetrical Γ-models, the HGM effectively mitigates the inaccuracies and biases of simplified models. This model balances the accuracy of the equivalent Π-model with the linearity of the short-line and Γ-models. An effective parameter estimation method is developed based on HGM, operating without requiring synchronized data. This method is applicable to both overhead lines and underground cables, and is particularly useful in the latter case, where shunt susceptance is more significant. By avoiding iterative solutions, the proposed method ensures convergence and eliminates the risk of multiple outcomes.**

***Index Terms*—Hybrid Γ-model, parameter estimation, unbalanced distribution feeders, unsynchronized measurements.**

I. Introduction

DISTRIBUTION systems are becoming increasingly complex and more in need of accurate knowledge of feeder parameters for reliable operation, control, and protection [1]. Traditionally, parameters of distribution network feeders (DNFs) have been estimated offline based on tower geometry and conductor electrical properties or by analyzing fault records. This data is not always readily available, and factors such as aging and ambient temperature may lead to parameter fluctuations [2]. This highlights the importance of online estimation methods that account for parameter variability.

The series impedance and shunt susceptance of DNFs can be estimated using measurements collected from the feeder terminals [3]. The solution becomes rather trivial by using synchronized voltage/current phasors collected at both terminals to determine the three-phase impedances of the feeder [4, 5]. Although Micro-Phasor Measurement Units (μPMUs) offer high accuracy, they are typically installed in limited locations. Financial and technical constraints limit their deployment, resulting in partial coverage of the DNFs. To address this challenge, research has focused on estimating feeder parameters using unsynchronized measurements without requiring the phase angle difference between terminals [2, 3]. A prevalent method for parameter estimation in DNFs involves developing nonlinear equations from active and reactive power measurements, which are then solved using iterative algorithms [3]. Iterative methods are prone to divergence and multiplicity of solutions. Alternatively, other methods utilize Artificial Intelligence (AI) to estimate feeder parameters using online unsynchronized measurements and offline trained models [2]. Unpredictability, training requirements, and biases are the common limitations of these AI-based methods.

The conventional simplified model of DNFs disregards feeder shunt susceptance, resulting in limited accuracy, particularly for underground cables [4]. In contrast, the Π-model introduces nonlinearity in the equations with respect to the parameters [6]. This motivates the development of a novel model for DNFs that maintains both simplicity and accuracy for parameter estimation.

The contributions of this letter can be summarized as follows:

- Proposing a Hybrid Γ-Model (HGM) that approaches the accuracy of the Π-model while preserving simplicity.
- Developing a generalized linear formula for estimating series impedance and shunt susceptance of unbalanced DNFs.
- Relying solely on unsynchronized measurements collected from local terminals for DNF parameter estimation.
- Addressing inaccuracies and biases present in common simplified models used in DNF studies.

II. Unbalanced Distribution Feeder Model

Different line models are designed to match specific characteristics and operational needs. Fig. 1 demonstrates a generalized schematic of commonly used models for representing DNFs [6, 7]. The nonzero coefficients in this schematic are α=0.5 and γ=0.5 for the equivalent Π-model, β=1 for the T model, α=1 for the Γ_ℓ-model, γ=1 for the Γ_r-model, all coefficients are zero for the short-line model. The Γ-model is a simplified representation of the feeder, incorporating both series impedance and shunt susceptance [7]. The left-hand Γ model (Γ_ℓ) positions the entire feeder susceptance at the sending end, while the right-hand Γ model (Γ_r) locates it at the receiving end of the feeder. Except for the equivalent Π-model, all other simplified models in Fig. 1 can introduce biases and inaccuracies. This letter proposes a novel HGM, which combines the asymmetrical Γ_ℓ- and Γ_r-models, as a more reliable model for DNFs. This novel model facilitates DNF parameter estimation while preserving accuracy.

Let the vectors $\boldsymbol{v}^s$ and $\boldsymbol{v}^r$ denote the voltage phasors at the sending (s) and receiving (r) terminals, respectively. The vectors $\boldsymbol{i}^s$ and $\boldsymbol{i}^r$ denote the sending end and receiving end current phasors of the feeder. $\boldsymbol{Z}^{sr}$ and $\boldsymbol{B}^{sr}$ denote the complex-valued series impedance and shunt susceptance matrices of feeder sr, respectively. KVL can be applied to the dashed boundary in Fig. 1. This boundary also forms a supernode where the total current entering equals the total current exiting, according to KCL. Using the equivalent Π-model for the feeder, the KVL and KCL equations are derived as follows:

Amin Nassaj and Sadegh Azizi are with the School of Electronic and Electrical Engineering, University of Leeds, Leeds, LS2 9JT, UK (e-mail: elana@leeds.ac.uk; s.azizi@leeds.ac.uk).

Ahmad Salehi Dobakhshari is with the Faculty of Engineering, University of Guilan, Rasht 4199613776, Iran (e-mail: salehi_ahmad@guilan.ac.ir).

Vladimir Terzija is with the School of Engineering, Newcastle University, Newcastle, NE1 7RU, UK (e-mail: vladimir.terzija@newcastle.ac.uk).

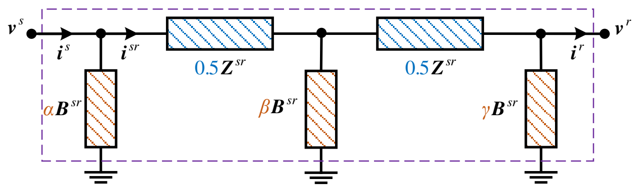

Fig. 1. Generalised schematic representing different DNF models.

$$\boldsymbol{v}^s = \boldsymbol{v}^r + \boldsymbol{Z}^{sr}\boldsymbol{i}^{sr} \tag{1}$$

$$\boldsymbol{i}^s = \tfrac{1}{2}\boldsymbol{B}^{sr}\boldsymbol{v}^s + \tfrac{1}{2}\boldsymbol{B}^{sr}\boldsymbol{v}^r + \boldsymbol{i}^r \tag{2}$$

where $\boldsymbol{i}^{sr}$ refers to the current across $\boldsymbol{Z}^{sr}$, represented by:

$$\boldsymbol{i}^{sr} = \boldsymbol{i}^s - \tfrac{1}{2}\boldsymbol{B}^{sr}\boldsymbol{v}^s = \boldsymbol{i}^r + \tfrac{1}{2}\boldsymbol{B}^{sr}\boldsymbol{v}^r \tag{3}$$

The equation for $\boldsymbol{i}^{sr}$ can be rewritten as:

$$\boldsymbol{i}^{sr} = \tfrac{1}{2}(\boldsymbol{i}^s + \boldsymbol{i}^r) - \tfrac{1}{4}\boldsymbol{B}^{sr}\Delta\boldsymbol{v}^{sr} \tag{4}$$

where $\Delta\boldsymbol{v}^{sr} = \boldsymbol{v}^s - \boldsymbol{v}^r$ is the voltage drop across the feeder. Given the short length of distribution feeders and the negligible voltage drops involved [8], the second term in (4) can be neglected. With this assumption, (1) can be rewritten as:

$$\boldsymbol{v}^s \approx \boldsymbol{v}^r + \tfrac{1}{2}\boldsymbol{Z}^{sr}\boldsymbol{i}^s + \tfrac{1}{2}\boldsymbol{Z}^{sr}\boldsymbol{i}^r \tag{5}$$

The equation above is essentially the KVL equation derived from the T-model of the feeder. Equations (2) and (5) represent a nearly accurate DNF model, based on the Π and T models.

Using the Γ_ℓ-model, on the other hand, the KVL and KCL equations can be approximated as

$$\boldsymbol{v}^s = \boldsymbol{v}^r + \boldsymbol{Z}^{sr}\boldsymbol{i}^r \tag{6}$$

$$\boldsymbol{i}^s = \boldsymbol{B}^{sr}\boldsymbol{v}^s + \boldsymbol{i}^r \tag{7}$$

Similarly, these equations using the Γ_r-model are as follows:

$$\boldsymbol{v}^s = \boldsymbol{v}^r + \boldsymbol{Z}^{sr}\boldsymbol{i}^s \tag{8}$$

$$\boldsymbol{i}^s = \boldsymbol{B}^{sr}\boldsymbol{v}^r + \boldsymbol{i}^r \tag{9}$$

Comparing (6)–(9) with (2) and (5), one can conclude that a nearly accurate DNF model can be derived by averaging (6) and (8) for KVL, and (7) and (9) for KCL, as follows:

$$\boldsymbol{v}^s = \tfrac{1}{2}(\boldsymbol{v}^r + \boldsymbol{Z}^{sr}\boldsymbol{i}^r) + \tfrac{1}{2}(\boldsymbol{v}^r + \boldsymbol{Z}^{sr}\boldsymbol{i}^s) \tag{10}$$

$$\boldsymbol{i}^s = \tfrac{1}{2}(\boldsymbol{B}^{sr}\boldsymbol{v}^r + \boldsymbol{i}^r) + \tfrac{1}{2}(\boldsymbol{B}^{sr}\boldsymbol{v}^s + \boldsymbol{i}^r) \tag{11}$$

Given the equivalence of (10) and (11) with (5) and (2), a simple yet nearly accurate DNF model can be derived by combining Γ_ℓ- and Γ_r-models, referred to as the HGM here. The equivalent circuit of the proposed HGM is shown in Fig. 2, where dependent voltage and current sources represent (10) and (11). Table I presents the neglected terms in the KVL and KCL equations using all other simplified models compared to the equivalent Π-model (where $\Delta\boldsymbol{i}^{sr} = \boldsymbol{i}^s - \boldsymbol{i}^r$). To assess the impact of feeder length on the accuracy of different models, a set of simulations are conducted on cable 692-675 in the IEEE 13-bus test feeder. The Mean Absolute Percentage Errors (MAPE) relative to feeder length are presented in Fig. 3, highlighting inaccuracies compared to the Π-model. Due to similar absolute errors in the Γ_ℓ- and Γ_r-models, only one is shown here, referred to as Γ model. The KVL inaccuracy of the HGM based on (5), which exhibits similar accuracy to the T model (as indicated in Table I), shows minimal variation with changes in feeder length and achieves a MAPE of 0.06% at a length of 10 km. Regarding KCL calculations, the HGM achieves accuracy comparable to the Π-model. Therefore, the proposed HGM maintains accuracy for both voltage and current variables while offering a system of linear equations suitable for parameter estimation.

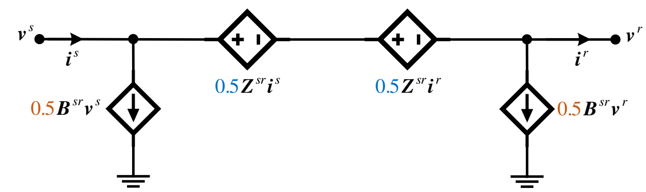

Fig. 2. Equivalent circuit of the proposed Hybrid Γ Model.

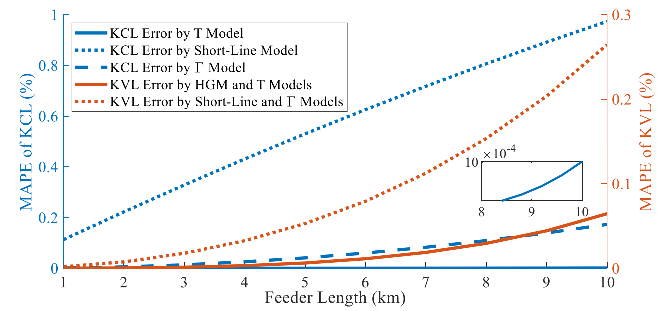

Fig. 3. Impact of feeder length on inaccuracy caused by different models.

TABLE I

COMPARISON BETWEEN DIFFERENT SIMPLIFIED DNF MODELS

Model	Type	Neglected terms in KCL	Neglected terms in KVL
Short Line	Linear Majorly Biased	$-\frac{1}{2}\boldsymbol{B}^{sr}(\boldsymbol{v}^s + \boldsymbol{v}^r)$	$-\frac{1}{2}\boldsymbol{Z}^{sr}\Delta\boldsymbol{i}^{sr} + \frac{1}{4}\boldsymbol{Z}^{sr}\boldsymbol{B}^{sr}\Delta\boldsymbol{v}^{sr}$
$\boldsymbol{\Gamma_\ell}$	Linear Majorly Biased	$\frac{1}{2}\boldsymbol{B}^{sr}\Delta\boldsymbol{v}^{sr}$	$-\frac{1}{2}\boldsymbol{Z}^{sr}\Delta\boldsymbol{i}^{sr} + \frac{1}{4}\boldsymbol{Z}^{sr}\boldsymbol{B}^{sr}\Delta\boldsymbol{v}^{sr}$
$\boldsymbol{\Gamma_r}$	Linear Majorly Biased	$-\frac{1}{2}\boldsymbol{B}^{sr}\Delta\boldsymbol{v}^{sr}$	$\frac{1}{2}\boldsymbol{Z}^{sr}\Delta\boldsymbol{i}^{sr} + \frac{1}{4}\boldsymbol{Z}^{sr}\boldsymbol{B}^{sr}\Delta\boldsymbol{v}^{sr}$
T	Nonlinear Minorly Biased	$-\frac{1}{4}\boldsymbol{Z}^{sr}\boldsymbol{B}^{sr}\Delta\boldsymbol{i}^{sr}$	$\frac{1}{4}\boldsymbol{Z}^{sr}\boldsymbol{B}^{sr}\Delta\boldsymbol{v}^{sr}$
HGM	Linear Minorly Biased	-	$\frac{1}{4}\boldsymbol{Z}^{sr}\boldsymbol{B}^{sr}\Delta\boldsymbol{v}^{sr}$

III. Parameter Estimation of Distribution Feeders

To leverage the accuracy of the proposed HGM in the parameter estimation problem, two linear systems of equations are derived to satisfy (10) and (11). Instead of directly using the average of (6)-(9) to obtain (10) and (11), equations (6) to (9) are modeled as a system of equations that yields results equivalent to (10) and (11) when the least-squares technique is applied. Using (6) and (9) within a single system of equations below represents the first terms in (10) and (11):

$$\begin{bmatrix}\boldsymbol{v}^s\\ \boldsymbol{i}^s\end{bmatrix} = \begin{bmatrix}\boldsymbol{I} & \boldsymbol{Z}^{sr}\\ \boldsymbol{B}^{sr} & \boldsymbol{I}\end{bmatrix}\begin{bmatrix}\boldsymbol{v}^r\\ \boldsymbol{i}^r\end{bmatrix} \tag{12}$$

Likewise, using (7) and (8) together accounts for the second terms in (10) and (11), yielding the following after adjustments:

$$\begin{bmatrix}\boldsymbol{v}^r\\ \boldsymbol{i}^r\end{bmatrix} = \begin{bmatrix}\boldsymbol{I} & -\boldsymbol{Z}^{sr}\\ -\boldsymbol{B}^{sr} & \boldsymbol{I}\end{bmatrix}\begin{bmatrix}\boldsymbol{v}^s\\ \boldsymbol{i}^s\end{bmatrix} \tag{13}$$

To linearly formulate a parameter estimation problem without the need for synchrophasors, voltage phase angles can be excluded from the variables at the sending or receiving terminal [9]. Given (12), dividing $\boldsymbol{v}^s$ by $\boldsymbol{i}^s$ gives:

$$\frac{v_p^s}{i_p^s} = \frac{|v_p^s|e^{j\delta_p^s}}{|i_p^s|e^{j\varphi_p^s+\delta_p^s}} = \frac{|v_p^s|}{|i_p^s|e^{j\varphi_p^s}} = \frac{v_p^r + \left(z_{pa}^{sr}i_a^r + z_{pb}^{sr}i_b^r + z_{pc}^{sr}i_c^r\right)}{i_p^r + \left(b_{pa}^{sr}v_a^r + b_{pb}^{sr}v_b^r + b_{pc}^{sr}v_c^r\right)} \tag{14}$$

where $|v_p^s|$ and $|i_p^s|$ denote the voltage and current magnitudes of phase $p = \{a, b, c\}$ at bus s, with δ_p^s as the voltage phase angle and φ_p^s as the phase angle difference between v_p^s and i_p^s.

Now, multiplying $e^{-j\delta_p^r}$ by both the numerator and denominator of (14) yields:

$$\frac{|v_p^s|}{|i_p^s|e^{j\varphi_p^s}} = \frac{|v_p^r|+\left(z_{pa}^{sr}\,|i_a^r|e^{j\varphi_a^r}\,o_{pa}^r+z_{pb}^{sr}\,|i_b^r|e^{j\varphi_b^r}\,o_{pb}^r+z_{pc}^{sr}\,|i_c^r|e^{j\varphi_c^r}\,o_{pc}^r\right)}{|i_p^r|e^{j\varphi_p^r}+\left(b_{pa}^{sr}\,|v_a^r|\,o_{pa}^r+b_{pb}^{sr}\,|v_b^r|\,o_{pb}^r+b_{pc}^{sr}\,|v_c^r|\,o_{pc}^r\right)} \quad (15)$$

where the operator $o_{pq}^r = e^{j(\delta_q^r-\delta_p^r)}$ denotes the voltage phase angle difference between phases q and p at bus r. The phase angle differences between the three-phase voltages (o_{pq}^r) and between voltages and currents (φ_p^r) in (15) can be measured locally [9, 10]. Since $\bar{v}_p = |v_p|$ and $\bar{\iota}_p = |i_p|e^{j\varphi_p}$, (15) can be reformulated as follows:

$$(\boldsymbol{Z}^{sr}\bar{\boldsymbol{\iota}}^r\boldsymbol{o}^r)\odot\bar{\boldsymbol{\iota}}^s - (\boldsymbol{B}^{sr}\bar{\boldsymbol{v}}^r\boldsymbol{o}^r)\odot\bar{\boldsymbol{v}}^s = \bar{\boldsymbol{v}}^s\odot\bar{\boldsymbol{\iota}}^r - \bar{\boldsymbol{v}}^r\odot\bar{\boldsymbol{\iota}}^s \quad (16)$$

where the operator $\odot$ represents the Hadamard product, which multiplies the corresponding elements of two vectors. To enable the satisfaction of (10) and (11) within the framework of the HGM, both (12) and (13) should be utilized in the problem. To this end, the division of $\boldsymbol{v}^r/\boldsymbol{i}^r$ in (13) results in:

$$(\boldsymbol{Z}^{sr}\bar{\boldsymbol{\iota}}^s\boldsymbol{o}^s)\odot\bar{\boldsymbol{\iota}}^r - (\boldsymbol{B}^{sr}\bar{\boldsymbol{v}}^s\boldsymbol{o}^s)\odot\bar{\boldsymbol{v}}^r = \bar{\boldsymbol{v}}^s\odot\bar{\boldsymbol{\iota}}^r - \bar{\boldsymbol{v}}^r\odot\bar{\boldsymbol{\iota}}^s \quad (17)$$

Given (16) and (17), two systems of linear equations can be derived using unsynchronized measurements. The generalized matrix form of using (16) and (17) for a set of n measurements is given by:

$$\begin{bmatrix} \boldsymbol{H}_{(1)}^i & \boldsymbol{H}_{(1)}^v \\ \boldsymbol{H}_{(2)}^i & \boldsymbol{H}_{(2)}^v \\ \vdots & \vdots \\ \boldsymbol{H}_{(n)}^i & \boldsymbol{H}_{(n)}^v \end{bmatrix} \begin{bmatrix} \boldsymbol{z}^{sr} \\ \boldsymbol{b}^{sr} \end{bmatrix} = \begin{bmatrix} \boldsymbol{u}_{(1)} \\ \boldsymbol{u}_{(2)} \\ \vdots \\ \boldsymbol{u}_{(n)} \end{bmatrix} \quad \equiv \quad \boldsymbol{Hx} = \boldsymbol{u} \quad (18)$$

The above system of linear equations is formed using only local unsynchronized measurements detailed in the Appendix. To solve (18), an adequate set of measurements should be used. To avoid an ill-conditioned coefficient matrix, at least 2, 4, and 6 sets of measurements are recommended for single-phase, two-phase, and three-phase feeders, respectively, under varying loading conditions [5].

Different methods can be used to estimate the state vector $\boldsymbol{x}$, while this study utilizes Weighted Least Squares (WLS):

$$\widehat{\boldsymbol{x}}_k = (\boldsymbol{H}_k^*\,\boldsymbol{W}_k\,\boldsymbol{H}_k)^{-1}\,\boldsymbol{H}_k^*\,\boldsymbol{W}_k\,\boldsymbol{u}_k \quad (19)$$

$$\boldsymbol{W}_k = diag(\boldsymbol{H}_k\,\widehat{\boldsymbol{x}}_{k-1} - \boldsymbol{u}_k)^{-2} \quad (20)$$

where $\boldsymbol{W}_k$ denotes the weight matrix at interval k. The proposed formula in (20) can be used to obtain a weight matrix by utilizing the mismatch between the previous estimates and current measurements. The effectiveness of the defined weights in (20) for WLS estimation is evaluated in the next section by comparing the results with those obtained from Ordinary Least Squares (OLS) using an identity weight matrix.

IV. Performance Evaluations

This section presents the simulation results obtained by applying the proposed parameter estimation formulation. The test system used for the experimentation is the IEEE 13-bus test feeder [11], modeled in PowerFactory 2022 SP1.

To evaluate the HGM's accuracy, simulations on underground cable 692-675 are conducted. Fig. 4 displays the Probability Density Function (PDF) of errors in calculating $\boldsymbol{i}^s$ and $\boldsymbol{v}^s$ across models, accounting for 0.1% measurement errors in 10,000 Monte Carlo simulations. As shown, using (8) and (9) in the Γ_ℓ-model and (10) and (11) in the Γ_r-model can increase standard deviations and biases. While using Γ_r- and Γ_ℓ-models separately can lead to inaccuracies and biases, combining these in HGM as represented by (10) and (11) effectively removes both concerns.

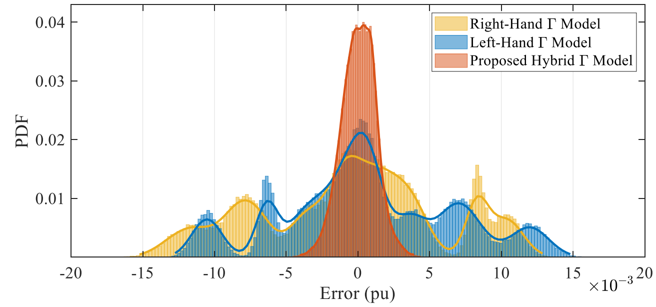

Fig. 4. Comparison between the accuracy of different Γ-based models.

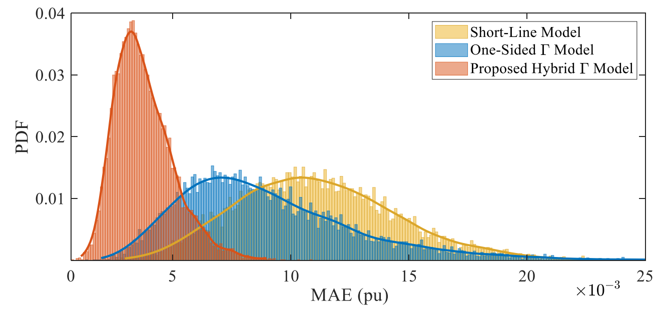

Fig. 5. Accuracy comparison of parameter estimations using different models.

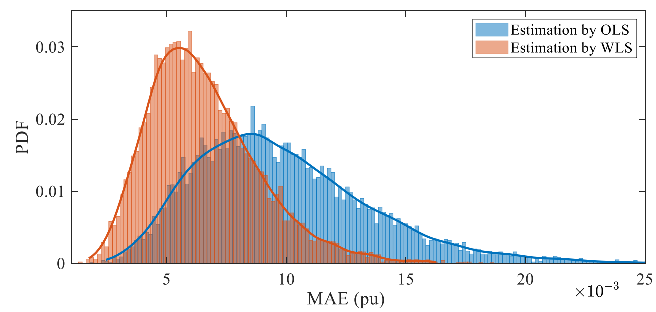

Fig. 6. Comparing the accuracy of OLS- and WLS-based estimations.

The next simulation compares parameter estimation results using the proposed HGM with the Γ_ℓ (as a one-sided Γ-model) and short-line models. Results from 10,000 Monte Carlo simulations on the same cable using six measurement sets are shown in Fig. 5, demonstrating the PDF of the Mean Absolute Error (MAE) for the three methods with 0.1% and 0.3% errors in voltage and current measurements, respectively. Fig. 5 shows the distribution of the MAE of the estimated series impedance and shunt susceptance in rectangular form. The proposed model yields higher accuracy with a mean MAE of 3.79×10^{-3} pu, compared to 9.05×10^{-3} pu and 11.13×10^{-3} pu by the Γ_ℓ and short-line models, respectively. As can be seen, the proposed HGM can effectively reduce estimation inaccuracies.

The effectiveness of the WLS-based parameter estimation formulation is evaluated through simulations on the three-phase line 632-671, with voltage and current errors set at 0.3% and 0.5% across 10,000 Monte Carlo simulations. Fig. 6 shows the results from six measurement sets, indicating that the weights defined in (20) reduce inaccuracy. The mean MAE for WLS estimation is 6.55×10^{-3} pu, compared to 9.89×10^{-3} pu for OLS.

V. Conclusion

This letter proposes a novel Hybrid Γ-Model (HGM) that provides a near-accurate approximation for Distribution Network Feeders (DNFs) while ensuring linearity and simplicity. Based on the HGM, a linear parameter estimation method is developed for DNFs using unsynchronized terminal measurements. Eliminating the need for time synchronization makes the method low-demanding and practical for DNFs. The proposed method is particularly effective in the case of underground cables with significant shunt capacitance, reliably providing parameters without divergence or yielding multiple outcomes.

Appendix

The submatrices used in (18) are as follows:

$$\boldsymbol{H}^{i}=\begin{bmatrix} \vec{\imath}_a^s\,\vec{\imath}_a^r & \vec{\imath}_a^s\,\vec{\imath}_b^r\,\bar{o}_{ab}^r & \vec{\imath}_a^s\,\vec{\imath}_c^r\,\bar{o}_{ac}^r & 0 & 0 & 0 \\ 0 & \vec{\imath}_b^s\,\vec{\imath}_a^r\,\bar{o}_{ba}^r & 0 & \vec{\imath}_b^s\,\vec{\imath}_b^r & \vec{\imath}_b^s\,\vec{\imath}_c^r\,\bar{o}_{bc}^r & 0 \\ 0 & 0 & \vec{\imath}_c^s\,\vec{\imath}_a^r\,\bar{o}_{ca}^r & 0 & \vec{\imath}_c^s\,\vec{\imath}_b^r\,\bar{o}_{cb}^r & \vec{\imath}_c^s\,\vec{\imath}_c^r \\ \vec{\imath}_a^r\,\vec{\imath}_a^s & \vec{\imath}_a^r\,\vec{\imath}_b^s\,\bar{o}_{ab}^s & \vec{\imath}_a^r\,\vec{\imath}_c^s\,\bar{o}_{ac}^s & 0 & 0 & 0 \\ 0 & \vec{\imath}_b^r\,\vec{\imath}_a^s\,\bar{o}_{ba}^s & 0 & \vec{\imath}_b^r\,\vec{\imath}_b^s & \vec{\imath}_b^r\,\vec{\imath}_c^s\,\bar{o}_{bc}^s & 0 \\ 0 & 0 & \vec{\imath}_c^r\,\vec{\imath}_a^s\,\bar{o}_{ca}^s & 0 & \vec{\imath}_c^r\,\vec{\imath}_b^s\,\bar{o}_{cb}^s & \vec{\imath}_c^r\,\vec{\imath}_c^s \end{bmatrix}$$

$$\boldsymbol{H}^{v}=-\begin{bmatrix} \bar{v}_a^s\,\bar{v}_a^r & \bar{v}_a^s\,\bar{v}_b^r\,\bar{o}_{ab}^r & \bar{v}_a^s\,\bar{v}_c^r\,\bar{o}_{ac}^r & 0 & 0 & 0 \\ 0 & \bar{v}_b^s\,\bar{v}_a^r\,\bar{o}_{ba}^r & 0 & \bar{v}_b^s\,\bar{v}_b^r & \bar{v}_b^s\,\bar{v}_c^r\,\bar{o}_{bc}^r & 0 \\ 0 & 0 & \bar{v}_c^s\,\bar{v}_a^r\,\bar{o}_{ca}^r & 0 & \bar{v}_c^s\,\bar{v}_b^r\,\bar{o}_{cb}^r & \bar{v}_c^s\,\bar{v}_c^r \\ \bar{v}_a^r\,\bar{v}_a^s & \bar{v}_a^r\,\bar{v}_b^s\,\bar{o}_{ab}^s & \bar{v}_a^r\,\bar{v}_c^s\,\bar{o}_{ac}^s & 0 & 0 & 0 \\ 0 & \bar{v}_b^r\,\bar{v}_a^s\,\bar{o}_{ba}^s & 0 & \bar{v}_b^r\,\bar{v}_b^s & \bar{v}_b^r\,\bar{v}_c^s\,\bar{o}_{bc}^s & 0 \\ 0 & 0 & \bar{v}_c^r\,\bar{v}_a^s\,\bar{o}_{ca}^s & 0 & \bar{v}_c^r\,\bar{v}_b^s\,\bar{o}_{cb}^s & \bar{v}_c^r\,\bar{v}_c^s \end{bmatrix}$$

$$\boldsymbol{u}=\begin{bmatrix} \bar{v}_a^s\,\vec{\imath}_a^r-\bar{v}_a^r\,\vec{\imath}_a^s \\ \bar{v}_b^s\,\vec{\imath}_b^r-\bar{v}_b^r\,\vec{\imath}_b^s \\ \bar{v}_c^s\,\vec{\imath}_c^r-\bar{v}_c^r\,\vec{\imath}_c^s \\ \bar{v}_a^s\,\vec{\imath}_a^r-\bar{v}_a^r\,\vec{\imath}_a^s \\ \bar{v}_b^s\,\vec{\imath}_b^r-\bar{v}_b^r\,\vec{\imath}_b^s \\ \bar{v}_c^s\,\vec{\imath}_c^r-\bar{v}_c^r\,\vec{\imath}_c^s \end{bmatrix} \qquad \boldsymbol{z}^{sr}=\begin{bmatrix} z_{aa}^{sr} \\ z_{ab}^{sr} \\ z_{ac}^{sr} \\ z_{bb}^{sr} \\ z_{bc}^{sr} \\ z_{cc}^{sr} \end{bmatrix} \qquad \boldsymbol{b}^{sr}=\begin{bmatrix} b_{aa}^{sr} \\ b_{ab}^{sr} \\ b_{ac}^{sr} \\ b_{bb}^{sr} \\ b_{bc}^{sr} \\ b_{cc}^{sr} \end{bmatrix}$$

References

[1] I. Series, *Microgrids and active distribution networks*: The Institution of Engineering and Technology, 2009.

[2] N. C. Yang, R. Huang, and M. F. Guo, "Distribution feeder parameter estimation without synchronized phasor measurement by using radial basis function neural networks and multi-run optimization method," *IEEE Access,* vol. 10, pp. 2869-2879, 2022.

[3] R. Dutta, V. S. Patel, S. Chakrabarti, A. Sharma, R. K. Das, and S. Mondal, "Parameter estimation of distribution lines using SCADA measurements," *IEEE Transactions on Instrumentation and Measurement,* vol. 70, pp. 1-11, 2021.

[4] B. Das, "Estimation of parameters of a three-phase distribution feeder," *IEEE Transactions on Power Delivery,* vol. 26, no. 4, pp. 2267-2276, 2011.

[5] V. Milojević, S. Čalija, G. Rietveld, M. V. Ačanski, and D. Colangelo, "Utilization of PMU measurements for three-phase line parameter estimation in power systems," *IEEE Transactions on Instrumentation and Measurement,* vol. 67, no. 10, pp. 2453-2462, 2018.

[6] W. H. Kersting, *Distribution system modeling and analysis*: CRC Press, 2018.

[7] A. R. Al-Roomi, and M. E. El-Hawary, "M-model: a new precise medium-length transmission line model," IEEE Canadian Conference on Electrical and Computer Engineering (CCECE), 2020, pp. 1-6.

[8] Y. Zhang, and J. Wang, "Towards highly efficient state estimation with nonlinear measurements in distribution systems," *IEEE Transactions on Power Systems,* vol. 35, no. 3, pp. 2471-2474, 2020.

[9] A. Nassaj, A. A. Jahromi, K. Li, V. Terzija, and S. Azizi, "Fast linear state estimation for unbalanced distribution systems using hybrid measurements," *IEEE Transactions on Instrumentation and Measurement,* vol. 73, pp. 1-10, 2024.

[10] E. Caro, A. J. Conejo, and R. Minguez, "Power system state estimation considering measurement dependencies," *IEEE Transactions on Power Systems,* vol. 24, no. 4, pp. 1875-1885, 2009.

[11] "IEEE PES test feeder," Available: https://cmte.ieee.org/pes-testfeeders/resources/.